Society For Biomaterials

Tailoring of the dopamine coated surface with VEGF loaded heparin/poly-L-lysine particles for anticoagulation and accelerate *in situ* endothelialization

Yang Liu,[1] Jiang Zhang,[1] Jian Wang,[1] Yuan Wang,[1] Zheng Zeng,[1] Tao Liu,[2] Junying Chen,[1] Nan Huang[1]

[1]Key Laboratory of Advanced Technology of Materials, Ministry of Education, Southwest Jiaotong University, Chengdu 610031, People's Republic of China
[2]Jiangsu Provincial Key Laboratory for Interventional Medical Devices, Huaiyin Institute of Technology, Huai'an 223003, People's Republic of China

Received 27 May 2014; revised 11 September 2014; accepted 19 September 2014
Published online 14 October 2014 in Wiley Online Library (wileyonlinelibrary.com). DOI: 10.1002/jbm.a.35339

Abstract: Coronary artery disease is a great threat to human health and is the leading killer worldwide. Percutaneous coronary intervention is the most effective therapy; however, thrombus, and restenosis caused by endothelium injury continue to be problematic after treatment. It is widely accepted that surface biofunctional modification to improve blood compatibility and accelerate endothelialization may be an effective approach to prevent the occurrence of adverse cardiac events. In this study, novel VEGF-loaded heparin/poly-L-lysine (Hep/PLL) particles were developed and immobilized on a dopamine coated titanium surface. The size, distribution, zeta potential, and morphology of the prepared particles were subsequently characterized. The influence of changes in the surface physicochemical properties after particle immobilization was assessed for blood compatibility and cytocompatibility. Surface-modified VEGF-loaded particles significantly inhibited platelet adhesion and activation and were effective in promoting the proliferation and survival of endothelial progenitor cells and endothelial cells. Moreover, Hep/PLL particles were also beneficial for controlling the long-term release of VEGF, which may facilitate endothelium regeneration. In conclusion, VEGF-loaded Hep/PLL particles were successfully immobilized on the Ti surface, and the biocompatibility was significantly improved. This study demonstrates a potential application for the multifunctional modification of stent surfaces for clinical use. © 2014 Wiley Periodicals, Inc. J Biomed Mater Res Part A: 103A: 2024–2034, 2015.

Key Words: titanium, heparin, VEGF, dopamine, endothelialization

How to cite this article: Liu Y, Zhang J, Wang J, Wang Y, Zeng Z, Liu T, Chen J, Huang N. 2015. Tailoring of the dopamine coated surface with VEGF loaded heparin/poly-L-lysine particles for anticoagulation and accelerate *in situ* endothelialization. J Biomed Mater Res Part A 2015:103A:2024–2034.

INTRODUCTION

Percutaneous coronary intervention (PCI) treatment using a metal stent is the primary therapy for coronary artery diseases (CADs). The available materials for metal stents include 316L stainless steel (SS), titanium (Ti) alloys, and cobalt-chromium (Co-Cr) alloys.[1,2] However, due to the insufficient biocompatibility of bare metal stents (BMSs) and the inevitable vascular injury caused by the implantation and expansion of these BMSs, adverse cardiac events, such as thrombus and restenosis, may occur. Therefore, drug-eluting stents (DESs) loaded with anti-proliferative drugs were introduced to prevent restenosis and contribute to a 50–70% reduction of the in-stent restenosis rate compared to BMSs.[3] Currently, DESs account for over 90% of the entire coronary artery stent market in China. Although the data for DESs is encouraging, they play a passive role in endothelium regeneration,[4] resulting in an increased risk of late thrombus and restenosis.[5–7]

In addition to DESs, the biofunctional modification of stent surfaces to accelerate *in situ* endothelialization and reduce adverse events has been suggested as a promising approach. Surface heparinization is a commonly used method to improve the blood compatibility and cellular compatibility of cardiovascular devices.[8,9] The anticoagulation effect of heparin is primarily dependent on the interaction with antithrombin III (AT III), and this process significantly accelerates the inactivation of thrombin and other clotting factors.[10] In addition, clinical research demonstrated that heparin also acts as an effective

Additional Supporting Information may be found in the online version of this article.
Correspondence to: T. Liu; e-mail: 198610190214kof@163.com or J. Chen; e-mail: chenjy@263.net
Contract grant sponsor: Key Basic Research Program; contract grant number: 2011CB606204
Contract grant sponsor: National Natural Science Foundation of China; contract grant numbers: 31170916, 31470921
Contract grant sponsor: Fundamental Research Funds for the Central Universities; contract grant number: SWJTU11ZT11

drug for anti-immune inflammatory therapy. The multifunctional characteristics of heparin result from its high affinity binding to plasma proteins and cell membrane proteins, which prevent the inflammatory response via blocking selectin-mediated macrophages and neutrophils adhesion to endothelial cells (ECs).[11] The abundant sulfate and carboxylate groups contribute to the large negative charge of heparin, which mediates electrostatic interactions with specific proteins, including enzymes, pathogen proteins, protease/esterase inhibitors, cytokines and chemokines, through heparin binding sites.[12] Of these proteins, the combination of heparin and vascular endothelial growth factor (VEGF) has been used in tissue regeneration recently.[13] Although heparin is considered harmful to EC growth,[14,15] recent studies suggest that the adverse effects can be minimized or even reversed in an adequate heparin dosage range.[16]

The endothelium layer consists of a monolayer of quiescent phenotype ECs that line the inside of blood vessels and plays an important role in preventing thrombosis and maintaining the normal function of the blood vessel. Therefore, accelerating the endothelialization of the stent is necessary to prevent the occurrence of adverse cardiac events.[17] The recently discovered endothelial progenitor cells (EPCs) derived from the bone marrow have great potential for vascular injury healing. Under induced vascular injury, EPCs are mobilized into the blood flow and home to the lesion site,[18] where they participate in endothelium regeneration.[19] VEGF is one of the most important inducible factors associated with EPCs mobilization, homing, and differentiation. Yoshinori et al.[20] demonstrated that VEGF modified surfaces, together with arterial shear stress, may promote the oriented differentiation of EPCs to ECs. Chung et al.[21] showed that the VEGF-loaded heparinized nanoparticle-fibrin gel complexes markedly increased the angiogenic activity in animal subcutaneous implantation or ischemic hind limb models.

The combined use of heparin and VEGF results in a more efficient and long-term affect in endothelium regeneration. The commonly used method to incorporate heparin or VEGF into biomaterials is covalent immobilization and electrostatic assembling. The covalent method is usually stable, but the role of the functional groups and conformational change of biomolecules during chemical crosslinking may result in a decrease in the bioactivity. The electrostatic interaction may have a small influence on the biomolecule activity, but the insufficient binding force may allow the constructed functional layer to rapidly lose its efficiency. Recently, bio-inspired polydopamine coating has been widely used in surface modification because of its non-specific affinity to various substrates[22] and specific reactivity with biomolecules rich in amine or sulfhydryl groups.[23–25] Poh et al.[26] developed a simple method for the covalent immobilization of VEGF on a dopamine (DM)-coated titanium surface. Although the result was promising, the amine consumption may lead a decrease in VEGF bioactivity.

In a previous study, we developed a novel heparin/poly-L-lysine (PLL) particle and demonstrated that the heparin activity was maintained on the DM-coated surface.[16] A similar method was also used by Tan et al.,[27] but their protocol for particle preparation and the experimental system differed from our study. In this study, Hep/PLL particles were screened for VEGF loading, and the VEGF-loaded particle was covalently immobilized on DM-coated Ti surfaces. The physicochemical properties of the modified surface of the particles were examined. The binding density and release behavior of heparin and VEGF were quantitatively characterized. According to the hemocompatibility and cellular compatibility evaluation, we demonstrated that the VEGF-loaded particle modified surfaces significantly inhibited platelet adhesion and activation and promoted EC and EPC growth.

MATERIALS AND METHODS

Materials and reagents

Commercial high purity titanium (Ti) (Φ 10 mm, purity 99.5%, Baoji, China) was used as the substrate for the Ti plates. The plates were polished, sonicated with acetone, ethanol, and deionized water and finally dried at room temperature (RT). Low molecular weight heparin (≥160 U/mg) was purchased from Bio Science & Technology Company (Shanghai, CH). DM, PLL (MW 150,000∼300,000), toluidine blue O (TBO), rhodamine 123, 4′, 6-diamidino-2-phenylindole (DAPI), and mouse monoclonal anti-human p-selectin antibody were purchased from Sigma-Aldrich. Human VEGF was purchased from Pepro Tech. Medium 199 and α-Modified Eagle's Medium (α-MEM) for cell culture and proliferation assays were purchased from BD Biosciences (San Jose, CA). Activated partial thromboplastin time (APTT) kits for the anticoagulation time test were purchased from Sunbio, China. For PLL and Hep solution preparation, 0.01*M* phosphate buffered saline (PBS, pH 7.4) was used. All other reagents used in the experiments were of the highest analytical purity (>99.9%).

VEGF-loaded Hep/PLL particle preparation and immobilization

The schematic drawing and TEM images of VEGF-loaded Hep/PLL particles are shown in Figure 1. Briefly, the Ti samples were immersed in 2 mg/mL polydopamine solution (dissolved in 10 m*M* Tris buffer, pH = 8.5) and incubated at 20°C for 12 h. Next, polydopamine-coated Ti was ultrasonically washed with double distilled water. The above processes were repeated three times, such that a total of three polydopamine layers were grafted onto the sample surfaces, and the samples were marked Ti-DM. Then, equal volumes of 10 mg/mL Hep solution and 200 ng/mL VEGF solution were mixed together and incubated at 37°C for 1 h. Subsequently, the mixture was added dropwise to 0.5 mg/mL PLL solution with equal volumes under ultrasonic conditions to create the VEGF-loaded Hep/PLL particles. Finally, the Ti-DM samples were immersed into the above particle solution and incubated at 37°C for 24 h with gentle shaking, and the particle modified surface was labeled Ti-DM-NPV. Hep/PLL particles without VEGF were used as the control, and the modified surface was called Ti-DM-NP.

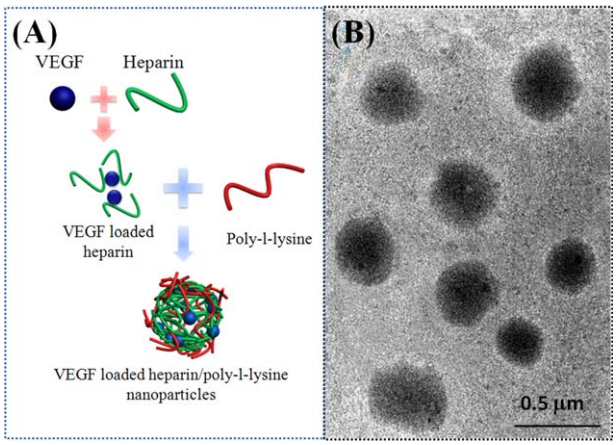

FIGURE 1. (A) Sketch drawing of VEGF-loaded particles preparation and (B) TEM images of prepared particles. [Color figure can be viewed in the online issue, which is available at wileyonlinelibrary.com.]

Particle size and zeta potential analysis

The mean size, particle dispersion index (PDI) and zeta potential of the VEGF-loaded Hep/PLL particles dispersed in PBS were determined by dynamic light scattering (DLS) using a ZETA-SIZER, MALVERN Nano-2S90 (Malvern, Malvern, UK).

FTIR

The changes in the surface the chemical structure after particle modification were monitored using an attenuated total reflectance Fourier transform-infrared instrument (ATR/FTIR, NICOLET 5700) with a scanning wavelength between 400 and 4000 cm^{-1}.

XPS

The surface elemental chemical composition was determined by X-ray photoelectron spectroscopy (XPS, XSAM800, Kratos, UK).

Atom force microscopy

The surface morphology after particle immobilization was characterized by atom force microscopy (AFM) (Nanowizard II, JPK Instruments, Berlin, Germany) in tapping mode. AFM was performed at RT, and image analysis was performed with the CSPM Imager software.

Water contact angle

The surface hydrophilicity was characterized by the water contact angle using a DSA100 (Kruüss, Hamburg, Germany) at RT and 60% relative humidity. For each sample, the mean value of the contact angle was calculated from at least three individual measurements.

Heparin binding density assay

The heparin binding density of the particle-immobilized surface was quantitatively characterized by TBO assay. The detailed experiment is described in our previous studies.[16] Ti and Ti-DM were used as blank controls.

Heparin and VEGF release assay

For the VEGF release assay, the particle modified samples were immersed in 0.5 mL PBS solution at 37°C and shaken (60–65 rpm) for 1, 3, 5, 7, 10, 14, 21, and 28 days in an air-tight centrifuge tube. A double-antibody sandwich ELISA was used to quantitatively evaluate the VEGF content, and the test was performed according to the instructions provided with the ELISA kit. VEGF-loaded particles were collected via 10 min of centrifugation at 15,000 rpm and the residual VEGF of the supernatant was detected by ELISA assay to indirectly calculate the total VEGF-loading amount. The cumulative release profile was normalized to the mean value of total VEGF-loading amount. For the heparin release assay, the release medium at each time point was collected and the TBO assay[16] was used to detect the heparin amount.

In vitro hemocompatibility evaluation

The fresh human whole blood used in the experiments was legally obtained from the central blood station of Chengdu, China. The analysis was performed within 12 h after blood donation.

Platelet adhesion. An *in vitro* platelet adhesion test was performed to evaluate the antithrombogenicity of the particle modified surface. First, fresh human whole blood was centrifuged at 1500 rpm for 15 min to collect the top layer of platelet rich plasma (PRP). Then, 50 μL PRP was added to each surface and incubated at 37°C for 2 h. Subsequently, the samples were rinsed three times with PBS to remove the weakly adsorbed platelets. Next, the adherent platelets were fixed in 2.5% glutaraldehyde at RT for 12 h, and subsequently, the samples were dehydrated with increasing alcohol (50%, 75%, 90%, 100%; $V_{Alcohol}/V_{UP}$) and dealcoholized in increasing isoamyl acetate concentrations (50%, 75%, 90%, 100%; $V_{Isoamyl\ acetate}/V_{Alcohol}$). Finally, the samples were vacuum dried, and the morphology of the adherent platelets was observed by SEM (Philips Quanta 200).

Platelet activation and p-selectin assay. p-Selectin expression was used as a marker of platelet activation induced by the surfaces. p-Selectin immunofluorescence staining was used to visually observe the activation. The staining procedures are described elsewhere.[16]

APTT. The APTT was tested to evaluate the influence of the sample surface on the bioactivity of the plasma clotting factors, IXa, Xa, and IIa. Fresh human whole blood was first centrifuged at 3000 rpm for 15 min to obtain platelet-poor plasma (PPP). Subsequently, 300 μL PPP was added to the samples and incubated at 37°C for 5 min. Then, 300 μL APTT agent was added and incubated at 37°C for 3 min. Then, 200 μL of the above mixture was removed and transferred to a test tube and followed by the addition of 100 μL 0.025*M* $CaCl_2$. The clotting time was measured with an automatic blood coagulation analyzer (ACL-200, Beckman Coulter, USA).

In vitro cytocompatibility evaluation

EPCs and ECs culture and seeding. EPCs were isolated from the bone marrow of Sprague-Dawley (SD) rats

TABLE I. The Size, PDI and Zeta Potential of Different Nanoparticles

Sample	Mean Size (nm)	PDI	Zeta Potential (mV)
NP	399	0.047	−31.7
NPV	334	0.062	−31.3

(Sichuan University, Chengdu, China) and cultured according to Li et al.[28] with modifications. Briefly, the bone marrow was extracted and resuspended with α-MEM containing 10% fetal bovine serum (FBS), and the resuspended cells were then seeded in a culture flask and incubated at 37°C with 95% air and 5% CO_2. The medium was changed every 2 days, and the cells were trypsinized for subculture at confluency. After one week, the cells were determined to be highly pure bone marrow stem cells (BMSCs), and the culture medium was replaced with α-MEM containing 10% FBS and 10 ng/mL VEGF. After 2 weeks of culture, the cells are identified as EPCs according to the cell morphology and specific markers.[16]

ECs were isolated from human umbilical veins and cultured. The human umbilical cord was thoroughly washed with sterile PBS to remove the residual blood. Then, 0.1% type II collagenase (Gibco BRL, USA) in medium 199 (M199) was injected and incubated at 37°C for 12 min. M199 with 10% FBS were used to stop digestion. The resuspended cells were collected by centrifugation at 1200 rpm for 10 min, then the supernatant was removed and the sediment was resuspended in M199 with 15% FBS and 20 μg/mL endothelial cell growth supplement (ECGS). Finally, the cell suspension was moved to a culture flask and incubated at 37°C under 5% CO_2.

Prior to cell seeding, the Ti and Ti-DM samples were sterilized with a high-pressure sterilizer at 120°C for 2 h. The PLL and VEGF solution were aseptically prepared, and the heparin solution was filtered with a Millipore filter. The particle preparation and immobilization were performed under aseptic condition. The EPCs and ECs were seeded at a concentration of 5×10^4 cells/per sample at 37°C. The medium used for cell seeding was similar to the cell culture but did not contain cytokines (VEGF or ECGS). The medium was changed every 2 days.

Fluorescence staining. Rhodamine 123 fluorescence staining was used to observe the morphology of adherent cells. After the predetermined time points (1 day, 3 days, and 5 days), the adherent cells were fixed in 2.5% glutaraldehyde for 12 h at RT. Then, the cells were stained at 37°C with rhodamine 123 (5 μg/mL, 50 μL per sample) for 20 min. After thoroughly washing with PBS, the samples were visualized by fluorescent microscopy (Zeiss, Germany). All procedures were performed in the dark.

EPC and EC proliferation: CCK-8. The cell counting kit-8 (CCK-8) (Dojindo, Japan) was used to evaluate the proliferation activity of different cells on each sample surface after 1, 3, and 5 days of culture. First, the samples were transferred to new 24-well plates, and then 400 μL fresh medium containing 10% CCK-8 reagent was added to each well and incubated at 37°C for an additional 3 h. Next, 150 μL culture medium was transferred into a 96-well plate and the absorbance was measured at 450 nm with a microplate reader.

Statistical analysis

At least three independent experiments were performed for the assay described above. The data are presented as the mean ± standard deviation (SD) One-way ANOVA in origin 8.0 was used to determine the statistical significance between and within groups. Values of $p < 0.05$ were considered significant.

RESULTS

Size and zeta potential of particles

According to our previous study, the formation of Hep/PLL particles is primarily mediated by intermolecular electrostatic interactions, and the concentration ratio of each biomolecule is critical to the size and stability of the formed particle, which indicates that the loading of VEGF affects the particle structure. Growth factors complexed with heparin promote a stronger interaction and more compact Hep/PLL particle formation.[29] As verification of the phenomenon, the size of the VEGF-loaded particles (NPV) was smaller than the non-VEGF loaded particles (NP), as shown Table I. However, the two types of particles share the same level of zeta potential. The absolute value of the zeta potential for both the NP and NPV were above 30 mV, which indicates that the particle system is moderately stable.[30] The polydispersity index (PDI) was used to reflect the uniformity of the formed particles. As shown in Table I, the PDI value of both the NP and NPV was smaller than 0.2, which indicates the excellent distribution of the prepared particles.

FTIR and XPS

FTIR analysis was used to detect the surface chemical group composition. As shown in Figure 2(A), compared to the Ti-DM, new peaks were observed after NP and NPV immobilization. A broad peak range from 3680 cm^{-1} to 3300 cm^{-1} is attributed to PLL-derived amine (—NH—, —NH_2—) and —OH stretching vibrations. The samples also presented peaks at 1666 cm^{-1} and 1565 cm^{-1}, which correspond to PLL-derived amide I (C═O) and II (C—N, N—H) bond stretching vibrations, respectively. The characteristic absorption peaks of heparin are observed at 1233 cm^{-1} and 1042 cm^{-1}, and correspond to the C—O—C and S═O bonds, respectively. XPS analysis was used to further understand the changes of the surface chemical compositions during particle immobilization. Figure 2(B) shows the XPS wide-scan spectra of different sample surfaces. After NP and NPV immobilization, new S2s (∼234.6 eV) and S2p (∼168.8 eV) peaks appeared in the spectrum after particle immobilization, which further confirmed the existence of heparin. The elemental percentage composition was calculated and listed in Table II, and compared to Ti-DM-NP, the sulfur (S)

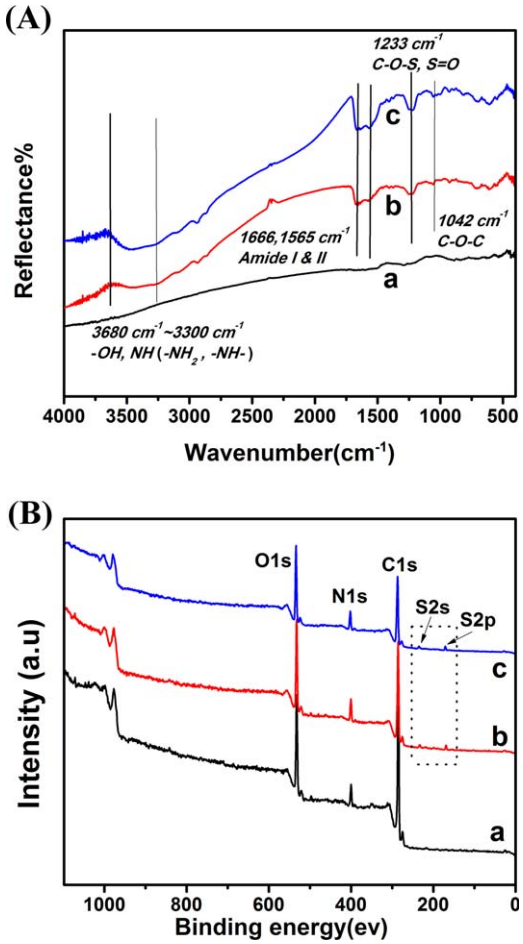

FIGURE 2. (A) FTIR spectra and (B) XPS wide-scan spectra of different samples. (a)∼(c) refers to Ti-DM, Ti-DM-NP, and Ti-DM-NPV, respectively. [Color figure can be viewed in the online issue, which is available at wileyonlinelibrary.com.]

content is higher on the NPV modified surface, which indicates that the heparin binding density on the Ti-DM-NPV surface may higher than on Ti-DM-NP.

AFM images of particles immobilized surface

The morphological changes after particle immobilization were determined by AFM assay. As shown in Figure 3, the control DM appears nearly uniformly flat. The particles on the NP and NPV modified surfaces were uniformly distributed with a mean size of 300∼400 nm, which corresponds to the with ZETA-SIZER results (Table I), and there is no significant difference in the morphology between the NP and NPV, indicating that VEGF loading may not affect particle structure.

Water contact angle

The surface hydrophilicity before and after particle immobilization was characterized by a water contact angle assay. According to Figure 4, after DM deposition, the water contact angle was increased from $52.7 \pm 2.89^\circ$ to $58.5 \pm 3.04^\circ$, suggesting that this was due to the exposure of hydrophobic groups, such as the benzene ring of DM. After NP and NPV immobilization, the water contact angle was dramatically decreased because of the hydrophilic groups in heparin and PLL, such as hydroxyl, amine, carboxyl, and sulfo groups. However, no significant difference was observed between NP and NPV.

Quantity of exposed heparin by TBO

Because the diffusion of the TBO reagent into the dense particles may be hindered, the heparin only exposed outermost layer is detected by TBO assay. As shown in Figure 5, the exposed heparin density on the NP immobilized surface was approximately 14.2 ± 1.7 μg/cm^2, which is consistent with our previous study.[16] However, the heparin exposed density increased to 16.7 ± 2.3 μg/cm^2 on the NPV modified surface. This may be partially due to the existence of VEGF, which contains amine groups that facilitate the interaction between the particles and DM coating. The Ti-DM surface showed a low false positive in TBO assay, which may be related to the non-specific adsorption of the test reagent and partial dissolution of DM in the NaOH/ethanol solution during the assay. Moreover, although the PLL content in the particles should be lower than heparin, it may neutralize the negative charges of heparin and cause some departure from the actual heparin amount.

In vitro release of heparin and VEGF

The cumulative release profile of heparin and VEGF at each time point was quantified by TBO assay and ELISA, respectively. Ti-DM-NP was used as a blank control. As shown in Figure 6, the VEGF release was similar heparin within 14 days, but slightly higher from 14 to 28 days. This result indicates that the VEGF release kinetics is highly correlated to the heparin release rate. According to our previous study, the heparin release profile was closely related to the particle structure due to the specific interaction between heparin and VEGF. It is reasonable to conclude that the specific 3D structure may indirectly regulate VEGF release. However, the difference between the heparin and VEGF release rate between 14 and 28 days may occur for the following two reasons: first, the residual particle has high stability and the long chain structure of heparin may contribute to decreasing the elution rate, whereas the VEGF that electrostatically binds to heparin may continual released from the particle[31,32]; and second, the released PLL may neutralize the heparin charges and cause the detected heparin amount to be lower than the actual heparin amount.

Blood compatibility evaluation

Platelet adhesion and activation. The adhesion and activation behavior of platelets on a biomaterial surface are highly

TABLE II. The Chemical Elemental Semi-quantitative Results on the Surface of Dopamine Coating and Nanoparticles

Samples	C%	N%	O%	S%	Ti%
Ti-DM	72.0	9.1	18.9	0.0	0.0
Ti-DM-NP	65.9	9.9	22.9	1.3	0.0
Ti-DM-NPV	65.4	9.8	23.1	1.7	0.0

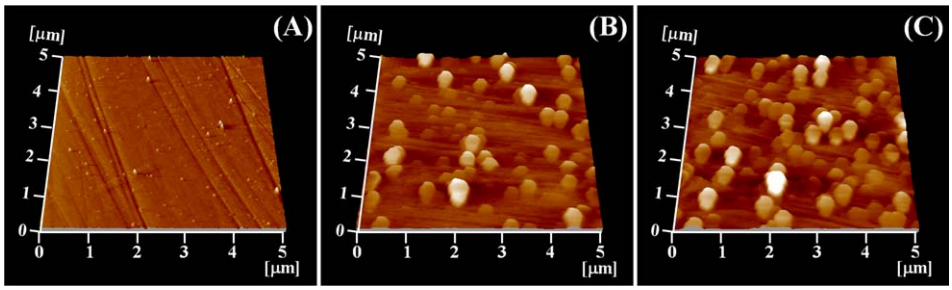

FIGURE 3. AFM images of the morphology of: (A) Ti-DM, (B) Ti-DM-NP, and (C) Ti-DM-NPV. [Color figure can be viewed in the online issue, which is available at wileyonlinelibrary.com.]

correlated to the occurrence of thrombus and other adverse events. SEM images (Fig. 7) showed that a large number of platelets aggregated on the Ti and Ti-DM surfaces and the adherent platelets presented will a fully spreading shape, which indicated high activation and poor blood compatibility. On the NP and NPV modified surface, although some platelets were adhered to the bare polydopamine area, the density of the adhered platelets was significantly decreased ($^*p < 0.05$) and had a round shape (Fig. 7). The p-selectin immunofluorescence staining result demonstrated that the expression of p-selectin on NP and NPV surface was significantly decreased compared to the Ti and Ti-DM surfaces (Fig. 7), which is attributed to the combined action of the exposed heparin and locally released heparin.

APTT. Activated partial thromboplastic time (APTT) assay, which is highly sensitive for heparin, was used to further evaluate the anticoagulation potency of particle-immobilized surfaces. As shown in Figure 8, the APTT value of PPP was ~31 s (normal range: 22–38 s), and the DM coating had no obvious influence on the clotting time. After NP and NPV immobilization, the APTT value was significantly prolonged to 66.4 ± 8.4 s and 74.7 ± 9.6 s, respectively. This was positive correlated with the heparin binding density result shown in Figure 5 and further indicates that VEGF promotes particle immobilization. This result indicates that the NP and NPV modified surfaces possess excellent anticoagulant efficiency.

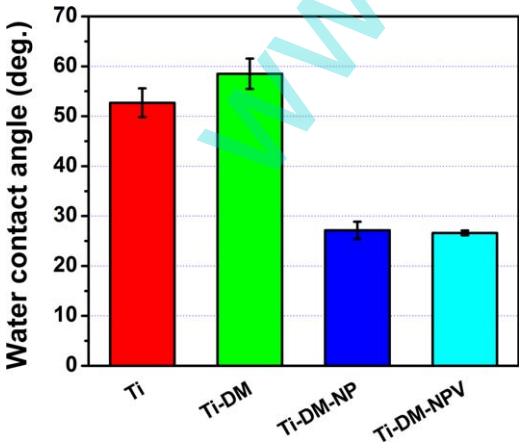

FIGURE 4. Water contact angle of different samples surface (mean ± SD, $N = 4$). [Color figure can be viewed in the online issue, which is available at wileyonlinelibrary.com.]

EPC and EC cellular compatibility evaluation

In vitro EC proliferation and migration and EPC proliferation was assessed to evaluate the endothelialization potential of modified surfaces. In this study, EPCs were identified by their typical cobblestone-like morphology and the specific expression of CD34, Flk-1 and vWF and were distinguished from ECs by proliferation (Supporting Information Fig. S1). According to Figure 9, after culture for 1, 3, and 5 days, EPC proliferation on NP-modified surfaces was not changed compared to Ti and Ti-DM. On the NPV modified surface, however, EPC proliferation was significantly increased compared to other groups ($^*p < 0.05$), and the adherent cells displayed typical cobble-stone morphology with outgrowth and formed a confluent cell layer on the sample surface at day 3.

As shown in Figure 10, compared to Ti, EC proliferation on the NP-modified surface was inhibited, which was different from the EPC growth profile. However, the ECs adhered to the NPV modified surface displayed significantly higher proliferation after culture for 3 and 5 days ($^*p < 0.05$). Notably, on Ti, Ti-DM, and Ti-DM-NP surfaces, the growth of ECs was greatly decreased and the adherent cells displayed shrinkage morphology. In comparison, the cells adhered

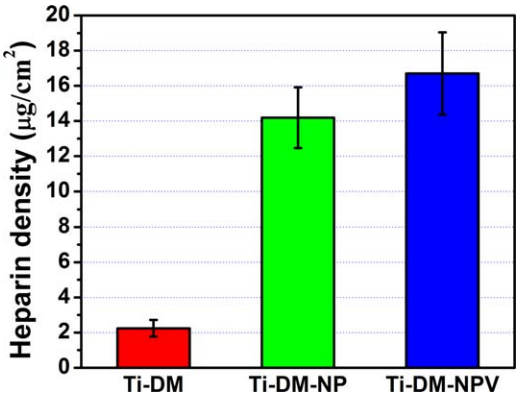

FIGURE 5. Quantitative characterization of heparin exposing density on NP and NPV immobilized surface by TBO assay (mean ± SD, $N = 6$). [Color figure can be viewed in the online issue, which is available at wileyonlinelibrary.com.]

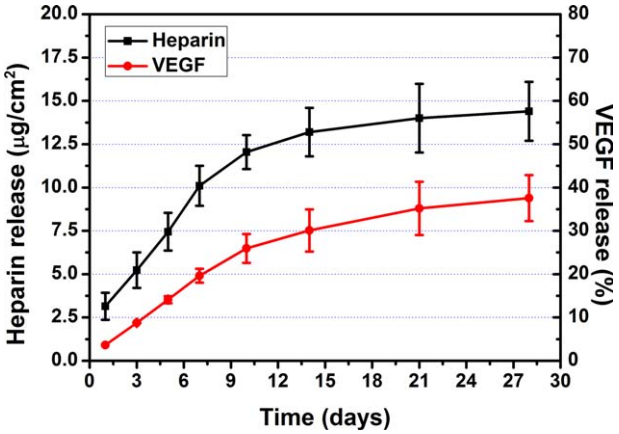

FIGURE 6. The release kinetics of heparin and VEGF from NPV modified surface. [Color figure can be viewed in the online issue, which is available at wileyonlinelibrary.com.]

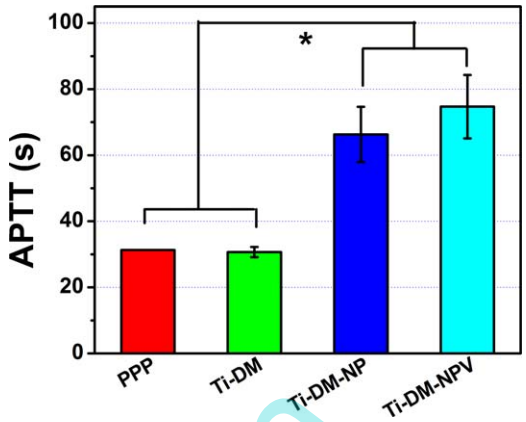

FIGURE 8. APTT on Ti-DM, Ti-DM-NP, and Ti-DM-NPV(mean ± SD, $N = 4$, $^*p < 0.05$). [Color figure can be viewed in the online issue, which is available at wileyonlinelibrary.com.]

onto the NPV modified surface maintained favorable growth morphology, indicating significant EC survival (Fig. 10).

Scarification is a common method to evaluate cell migration,[33] but is not appropriate for particle-immobilized surfaces due to the damage of surface properties during this process. Here, a new method is introduced and shown in Figure 11. Compared to Ti-DM, the NP-modified surface displayed no positive effects on EC migration. However, the migration distance of ECs on NPV-modified surface reached 858 ± 78 μm after 1 day, which was approximately 1.6 times higher than on the Ti-DM surface and 1.8 times higher compared with the Ti-DM-NP surface. This result suggests that the combination of VEGF may greatly facilitate *in situ* endothelialization.

DISCUSSION

A single functional modification of the coronary artery stent surface is insufficient to meet the clinical requirements for biocompatibility. Currently, surface multifunctional modification to construct a biomimetic microenvironment for selective direction of platelets and vascular cells behavior has become an attractive target. Numerous approaches, such as layer-by-layer assembly or co-immobilization, have been used for surface multifunction environment construction.[34] However, the correct combination of surface biological properties and architecture have not been identified. An important limitation is to effectively conjugate biofunctional molecules to inorganic surfaces while maintaining sufficient binding density, bioactivity, and durability. The emergence of polydopamine coating significantly facilitates the

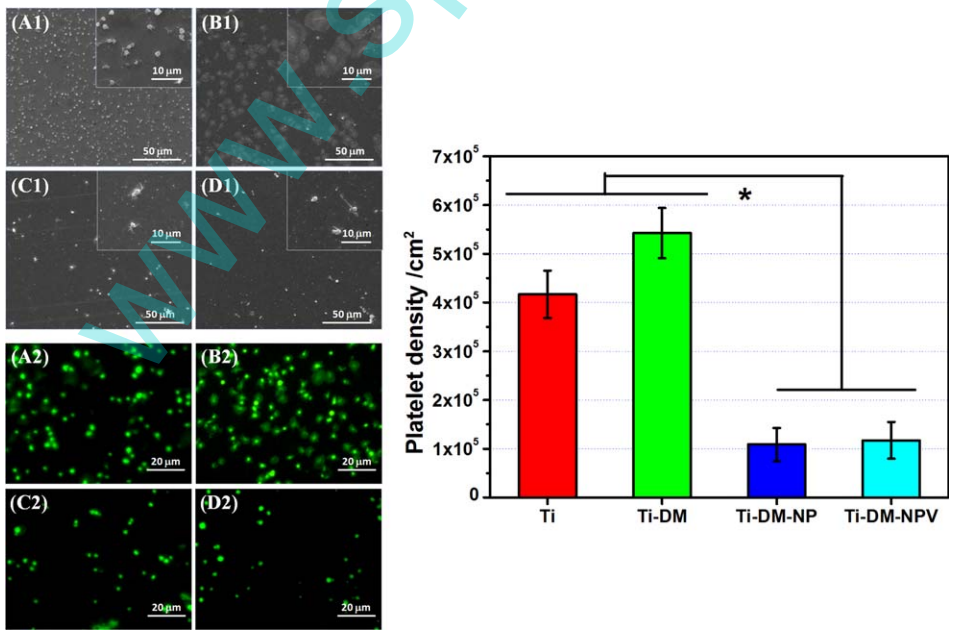

FIGURE 7. Right: Platelet counting result. (mean ± SD, $N = 6$, $^*p < 0.05$). Left: (A1)∼(D1) represent the SEM images of adherent platelets on various substrates; (A2)∼(D2) refers to p-selectin immunofluorescence staining of adherent platelets on various substrates. (A) Ti, (B) Ti-DM, (C) Ti-DM-NP, (D) Ti-DM-NPV. [Color figure can be viewed in the online issue, which is available at wileyonlinelibrary.com.]

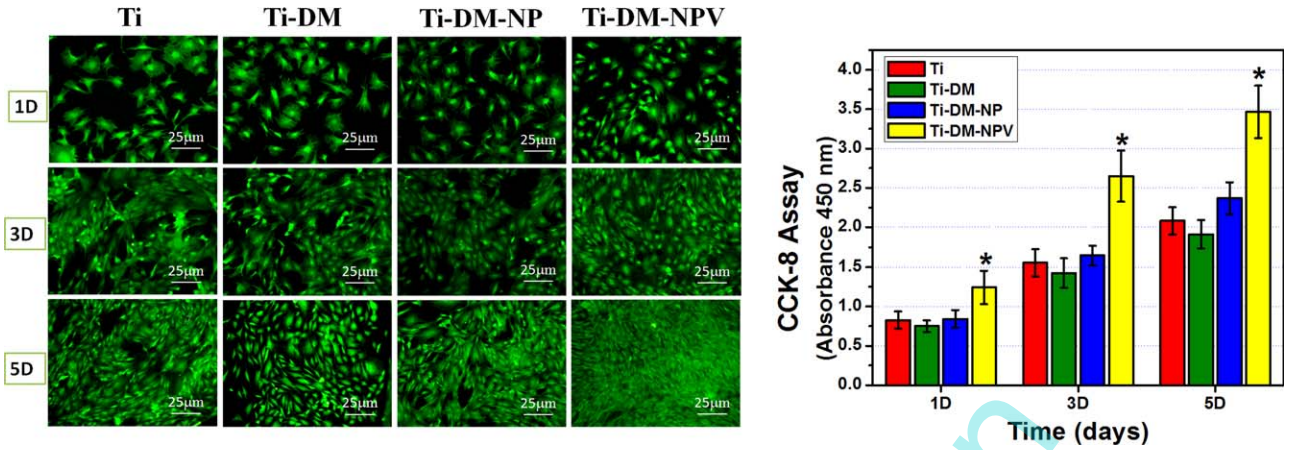

FIGURE 9. Rhodamine 123 fluorescence staining of adherent EPCs on different sample surfaces and related CCK-8 result after 1, 3, and 5 days of culture. [Color figure can be viewed in the online issue, which is available at wileyonlinelibrary.com.]

immobilization of amino or sulfhydryl group containing molecules to material surfaces.[22] However, for blood contact surface modification, improving the hemocompatibility of the polydopamine coating should be the primary task.

Heparin as an anticoagulant has been used clinically for over 70 years. In recent decades, heparin was shown to inhibit SMC over-proliferation and inflammation, and improve endothelialization.[35–37] The multifunctional property of heparin depends on the intermolecular interactions with various heparin-binding proteins, including complement protein,[38] cell membrane ligands,[39] and endothelium growth factors. The incorporation of heparin into biomaterials to improve hemocompatibility, control drug delivery and direct cellular behavior is now an area of focus. However, for surface heparinization of cardiovascular devices, covalent conjugation continues to be the most commonly used method, which may destroy the conformation of the heparin and decrease the anticoagulation potency. In our previous study, novel hep/PLL particles were developed for surface heparinization of DM coating, and the structure and binding density of these particles can be controlled.[16] In the present study, the specific interaction between heparin and VEGF was utilized[21,40] and a novel VEGF-loaded hep/PLL particle was prepared and immobilized on DM coated Ti surface, to control the long-term release of VEGF and effectively accelerate endothelialization based on hemocompatibility.

VEGF-loaded hep/PLL particles with favorable uniformity and stability were prepared with a specific process. The success of immobilization on DM-coated particles was monitored by FTIR, XPS, and AFM assay. Furthermore, the heparin and VEGF release behavior was well controlled on the NPV modified surface (Fig. 6), and combined with our recent study,[41] the result indicates that the superior stability of the particles may contribute to controlling the biomolecule delivery. Many studies have also demonstrated that the heparin binding proteins bind to heparin with a dissociation constant of up to 10^{-6}–$10^{-9}M$ K_D[42]; therefore, the specific interaction between heparin and VEGF may also be beneficial for controlling VEGF release. In conclusion, under the combined action of heparin and the specific 3D structure of the particles, VEGF showed controlled and sustained release behavior within 28 days (Fig. 6). High levels of

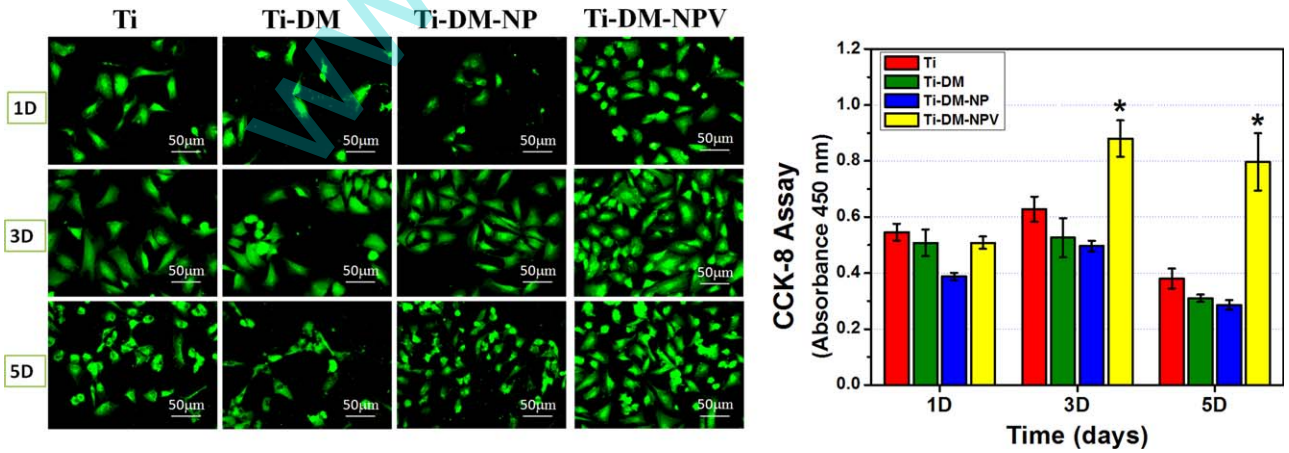

FIGURE 10. Rhodamine 123 fluorescence staining of adherent ECs on different sample surfaces and related CCK-8 result after 1, 3, and 5 days of culture. [Color figure can be viewed in the online issue, which is available at wileyonlinelibrary.com.]

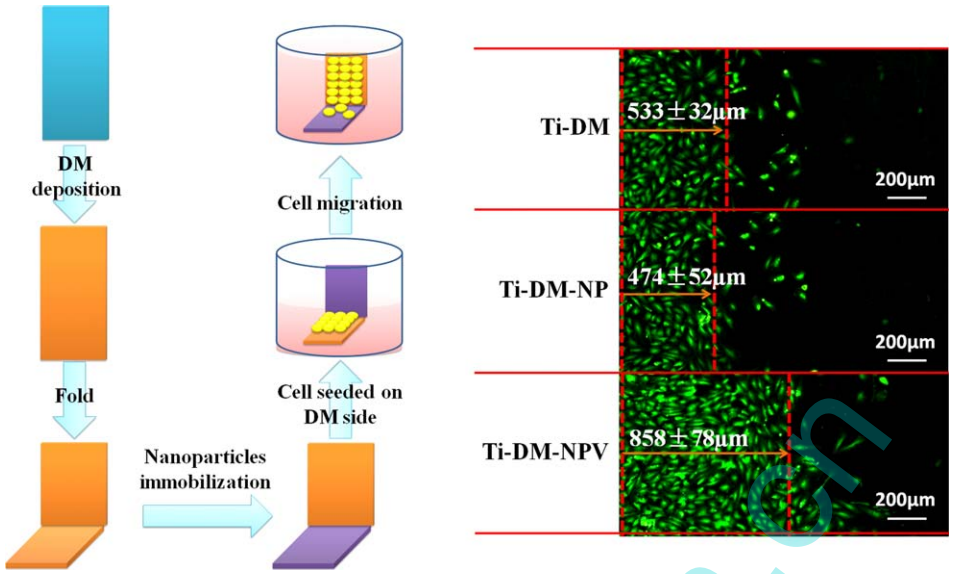

FIGURE 11. Migration assay of ECs from DM coated surface to Ti-DM, Ti-DM-NP, and Ti-DM-NPV surfaces. Left: Schematic drawing of migration assay. Right: rhodamine fluorescence staining result. The migration distance was calculated from at least nine images. [Color figure can be viewed in the online issue, which is available at wileyonlinelibrary.com.]

VEGF in the local microenvironment may be detrimental to vascular injury healing and even promote the formation of malformed vessels.[43] Therefore, the present study may provide a method for the controlled delivery of cytokines.

For the surface modification of blood contact materials, improving the hemocompatibility is the most basic requirement. Heparin is a heterogeneous mix of mucopolysaccharides, which may bind to the anticoagulant antithrombin III (AT III), thereby effectively enhancing the blocking effect to thrombin and other activated clotting factors, such as Xa, IXa, XIa, and XIIa.[44] The anticoagulant potency of heparinized surface primarily depends on the heparin binding density and activity. Yang et al.[35] demonstrated that surface binding to ~280 ng/cm^2 heparin (bioactivity well retained) is sufficient to provide favorable anticoagulation. In this study, the heparin binding density of the NP- and NPV-modified surface reached 14.2 ± 1.7 μg/cm^2 and 16.7 ± 2.3 μg/cm^2, respectively (Fig. 5). The APTT results showed that the clotting times of particles on the immobilized surface were prolonged by 80~100 s (Fig. 8), and this prolongation is positively correlated with heparin binding density and indicates significant inhibition of the activation of plasma clotting factors. *In vitro* platelet adhesion and activation also demonstrated that both the NP- and NPV-modified surface effectively inhibit platelet adhesion and activation. These results suggest that the heparin embedded in particles maintains favorable anticoagulation activity and that the hemocompatibility of the modified surface was greatly improved.

Cell adhesion and proliferation on material surfaces largely depends on the surface physical and chemical properties, such as hydrophilicity, topography, and ligand density. According to our previous study,[16] the heparin binding density of Hep/PLL particle modified surface at the range of 3~7 μg/cm^2 results in excellent hemocompatibility and protection from SMC over-proliferation, but accelerates endothelialization. However, EC growth may be inhibited when the heparin density is greater than 10 μg/cm^2. In this study, the NP-modified surface had several beneficial effects on EC migration (Fig. 11) and EPC growth (Fig. 9). EC proliferation, however, was inhibited (Fig. 10). This was attributed to the large negatively charged heparin, which blocks important intercellular signaling pathways closely related to cell adhesion, proliferation and survival.[45,46] However, on the NPV-modified surface, the adhesion, and proliferation of EPCs and ECs were significantly increased (Figs. 9 and 10). This was partially due to the positive effect of VEGF on cell proliferation and survival.[47] Furthermore, the interaction between VEGF and heparin may also contribute to a prolonged half-life and activity of VEGF, and may decrease the negative effect of heparin on cell growth.

Surface multifunctional modification using simple but effective methods is the primary objective of stent development, but the bioactivity and density of functional biomolecules should be precisely controlled. In this study, the specific intermolecular interactions among heparin, VEGF, and PLL, were used to successfully develop a novel type of VEGF-loaded heparin/PLL particle for surface anticoagulation and to accelerate endothelialization modification of DM-coated Ti. The bioactivity of VEGF and heparin was retained, and the NPV-modified surface presented superior anticoagulation properties and promoted endothelialization *in vitro*. However, the *in vivo* induction of endothelium regeneration, and maintenance of long-term biocompatibility was difficult to predict and further studies are necessary.

CONCLUSIONS

Based on our previous study, a novel VEGF loaded hep/PLL particles was developed and immobilized on a DM-coated Ti surface. The specific structure of the particles and intermolecular interactions between heparin and VEGF contribute

to the long-term uniform release of VEGF. Both NP- and NPV-modified surfaces displayed superior hemocompatibility, but NP inhibits EC proliferation. VEGF loading effectively promoted EC migration and growth, and EPC proliferation. This study identifies a promising approach for surface multifunctional modification of cardiovascular stents tailored for platelet and vascular cell behavior.

REFERENCES

1. Rajesh T, Wahid K, Abraham JD. Eluting combination drugs from stents. Int J Pharm 2013;454:4–10.
2. Rigberg D, Tulloch A, Chun Y, Mohanchandra KP, Carman G, Lawrence P. Thin-film nitinol (NiTi): A feasibility study for a novel aortic stent graft material. J Vasc Surg 2009;50:375–380.
3. David MM, Fergal JB. Drug-eluting stents for coronary artery disease: A review. Med Eng Phys 2011;33:148–163.
4. Joner M, Nakazawa G, Finn AV, Quee SC, Coleman L, Acampado E, Wilson PS, Skorija K, Cheng Q, Xu X, Gold HK, Kolodgie FD, Virmani R. Endothelial cell recovery between comparator polymer-based drug-eluting stents. J Am Coll Cardiol 2008;52: 333–342.
5. Finn AV, Joner M, Nakazawa G, Kolodgie F, Newell J, John MC, Gold HK, Virmani R. Pathological correlates of late drug-eluting stent thrombosis: Strut coverage as a marker of endothelialization. Circulation 2007;115:2435–2441.
6. Joner M, Finn AV, Farb A, Mont EK, Kolodgie FD, Ladich E, Kutys R, Skorija K, Gold HK, Virmani R. Pathology of drug-eluting stents in humans: Delayed healing and late thrombotic risk. J Am Coll Cardiol 2006;48:193–202.
7. Nakazawa G, Finn AV, Joner M, Ladich E, Kutys R, Mont EK, Gold HK, Burke AP, Kolodgie FD, Virmani R. Delayed arterial healing and increased late stent thrombosis at culprit sites after drug eluting stent placement for acute myocardial infarction patients: An autopsy study. Circulation 2008;118:1138–1145.
8. Ryan AH, Robert VL, Michele CJ, Josephine BA, Karen AL, Guillermo A. The blood and vascular cell compatibility of heparin-modified ePTFE vascular grafts. Biomaterials 2013;34:30–41.
9. Li GC, Yang P, Qin W, Maitz MF, Zhou S, Huang N. The effect of coimmobilizing heparin and fibronectin on titanium on hemocompatibility and endothelialization. Biomaterials 2011;32:4691–4703.
10. Rosenberg RD, Damus PS. The role of heparin in the thrombin-antithrombin III reaction. J Biol Chem 1976;175:153–159.
11. Young, E. The anti-inflammatory effects of heparin and related compounds. Thromb Res 2008;122:743–752.
12. Capila I, Linhardt RJ. Heparin–protein interactions. Angew Chem Int Ed 2002;41:390–412.
13. Kharkar PM, Kiick KL, Kloxin AM. Designing degradable hydrogels for orthogonal control of cell microenvironments. Chem Soc Rev 2013;42:7335–7372.
14. Cariou R, Harousseau JL, Tobelem G. Inhibition of human endothelial cell proliferation by heparin and steroids. Cell Biol Int Rep 1988;12:1037–1047.
15. Khorana AA, Sahni A, Altland OD, Francis CW. Heparin inhibition of endothelial cell proliferation and organization is dependent on molecular weight. Arterioscler Thromb Vasc Biol 2003;23:2110–2115.
16. Liu T, Liu Y, Chen Y, Liu S, Maitz MF, Wang X, Zhang K, Wang J, Wang Y, Chen J, Huang N. Immobilization of heparin/poly-l-lysine nanoparticles on dopamine-coated surface to create a heparin density gradient for selective direction of platelet and vascular cells behavior. Acta Biomater 2014;10:1940–1954.
17. Serruys PW, Kutryk MJB, Ong ATL. Coronary-artery stents. N Engl J Med 2006;354:483–495.
18. Asahara T, Murohara T, Sullivan A, Silver M, van der Zee R, Li T, Witzenbichler B, Schatteman G, Isner JM. Isolation of putative progenitor endothelial cells for angiogenesis. Science 1997;275: 964–967.
19. Padfield GJ, Newby DE, Mills NL. Understanding the role of endothelial progenitor cells in percutaneous coronary intervention. J Am Coll Cardiol 2010;55:1553–1565.
20. Suzuki Y, Yamamoto K, Ando J, Matsumoto K, Matsuda T. Arterial shear stress augments the differentiation of endothelial progenitor. Biochem Biophys Res Commun 2012;424:91–97.
21. Chung YI, Kim SK, Lee YK, Park SJ, Cho KO, Yuk SH, Tae G, Kim YH. Efficient revascuarization by VEGF administration via heparin-functionalized nanoparticle–fibrin complex cells adhered to VEGF-bound surfaces. J Control Release 2010;143:282–289.
22. Lee H, Dellatore SM, Miller WM, Messersmith PB. Mussel-inspired surface chemistry for multifunctional coatings. Science 2007;318: 426–430.
23. Luo R, Tang L, Wang J, Zhao Y, Tu Q, Weng Y, Shen R, Huang N. Improved immobilization of biomolecules to quinone-rich polydopamine for efficient surface functionalization. Colloids Surf B Biointerfaces 2013;106:66–73.
24. Lee YB, Shin YM, Lee J, Jun I, Kang JK, Park JC, Shin H. Polydopamine-mediated immobilization of multiple bioactive molecules for the development of functional vascular graft materials. Biomaterials 2012;33:8343–8352.
25. Chen S, Li X, Yang Z, Zhou S, Luo R, Maitz MF, Zhao Y, Wang J, Xiong K, Huang N. A simple one-step modification of various materials for introducing effective multi-functional groups. Colloid Surf B Biointerfaces 2014;113:125–133.
26. Poh CK, Shi Z, Lim TY, Neoh KG, Wang W. The effect of VEGF functionalization of titanium on endothelial cells in vitro. Biomaterials 2010;31:1578–1585.
27. Tan Q, Tang H, Hu J, Hu Y, Zhou X, Tao Y, Wu Z. Controlled release of chitosan/heparin nanoparticle-delivered VEGF enhances regeneration of decellularized tissue-engineered scaffolds. Int J Nanomed 2011;6:929–942.
28. Li QL, Huang N, Chen C, Chen JL, Xiong KQ, Chen JY, You TX, Jin J, Liang X. Oriented immobilization of anti-CD34 antibody on titanium surface for self-endothelialization induction. J Biomed Mater Res A 2010;94:1283–1293.
29. Park KH, Kim H, Na K. Neuronal Differentiation of PC12 cells cultured on growth factor-loaded nanoparticles coated on PLGA microspheres. J Microbiol Biotechnol 2009;19:1490–1495.
30. Hanaor D, Michelazzi M, Leonelli C, Sorrell CC. The effects of carboxylic acids on the aqueous dispersion and electrophoretic deposition of ZrO2. J Eur Ceram Soc 2012;32:235–244.
31. Freeman I, Kedem A, Cohen S. The effect of sulfation of alginate hydrogels onthe specific binding and controlled release of heparin-binding proteins. Biomaterials 2008;29:3260–3268.
32. Chu H, Johnson NR, Mason NS, Wang Y. A [polycation: Heparin] complex releases growth factors with enhanced bioactivity. J Control Release 2011;150:157–163.
33. Madri JA, Stenn KS. Aortic endothelial cell migration. I. Matrix requirements and composition. Am J Pathol 1982; 106:180–186.
34. Meng S, Liu Z, Shen L, Guo Z, Chou LL, Zhong W, Du Q, Ge J. The effect of a layer-by-layer chitosan-heparin coating on the endothelialization and coagulation properties of a coronary stent system. Biomaterials 2009;30:2276–2287.
35. Yang Z, Tu Q, Wang J, Huang N. The role of heparin binding surfaces in the direction of endothelial and smooth muscle cell fate and re-endothelialization. Biomaterials 2012;33:6615–6625.
36. Brown RA, Leung E, Kankaanranta H, Moilanen E, Page CP. Effects of heparin and related drugs on neutrophil function. Pulm Pharmacol Ther 2012;25:185–192.
37. Lever R, Smailbegovic A, Page CP. Locally available heparin modulates inflammatory cell recruitment in a manner independent of anticoagulant activity. Eur J Pharmacol 2010;630:137–144.
38. Weiler JM, Edens RE, Linhardt RJ, Kapelanski DP. Heparin and modified heparin inhibit complement activation in vivo. J Immunol 1992;148:3210–3215.
39. Nelson RM, Cecconi O, Roberts WG, et al. Heparin oligosaccharides bind L-and P-selectin and inhibit acute inflammation. Blood 1993;82:3253–3258.
40. Lauten EH, VerBerkmoes J, Choi J, Jin R, Edwards DA, Loscalzo J, Zhang YY. Nanoglycan complex formulation extends VEGF retention time in the lung. Biomacromolecules 2010;11:1863–1872.
41. Liu T, Zeng Z, Liu Y, Wang J, Maitz MF, Wang Y, Liu S, Chen J, Huang N. Surface modification with dopamine and heparin/poly-l-lysine nanoparticles provides a favorable release behavior for the

healing of vascular stent lesions. ACS Appl Mater Interfaces 2014; 6:8729–8743.
42. Cardin AD, Jackson RL, Sparrow DA, Sparrow JT. Interaction of glycosaminoglycans with lipoproteins. Ann NY Acad Sci 1989; 556:186–193.
43. Ehrbar M, Djonov VG, Schnell C, Tschanz SA, Martiny-Baron G, Schenk U, Wood J, Burri PH, Hubbell JA, Zisch AH. Cell-demanded liberation of VEGF121 from fibrin implants induces local and controlled blood vessel growth. Circ Res 2004;94:1124–1132.
44. Hirsch J, Anand S, Halperin J, Fuster V. Mechanism of action and pharmacology of unfractionated heparin. Anterioscler Thromb Vasc Biol 2001; 21:1094–1106.
45. Li X, Zheng Z, Li X, Ma X. Unfractionated heparin inhibits lipopolysaccharide-induced inflammatory response through blocking p38 MAPK and NF-κB activation on endothelial cell. Cytokine 2012;60:114–121.
46. Ettelaie C, Fountain D, Collier ME, Elkeeb AM, Xiao YP, Maraveyas A. Low molecular weight heparin downregulates tissue factor expression and activity by modulating growth factor receptor-mediated induction of nuclear factor-κB. Biochim Biophys Acta 2011;1812:1591–1600.
47. Hutchings H, Ortega N, Plouêt J. Extracellular matrix-bound vascular endothelial growth factor promotes endothelial cell adhesion, migration, and survival through integrin ligation. The FASEB J 2003;7:1520–1522.